Southern Ocean deep convection as a driver of Antarctic warming events

J.B. Pedro[1,*], T. Martin[2,*], E. J. Steig[3], M. Jochum[1], W. Park[2], & S.O. Rasmussen[1]

[1]Center for Ice and Climate, Niels Bohr Institute, University of Copenhagen, Denmark

[2]GEOMAR Helmholtz Centre for Ocean Research Kiel, Kiel, Germany

[3]University of Washington, Seattle, WA, USA

*Corresponding authors with equal contributions to the study: jpedro@nbi.ku.dk, tomartin@geomar.de

This article has been accepted for publication and undergone full peer review but has not been through the copyediting, typesetting, pagination and proofreading process which may lead to differences between this version and the Version of Record. Please cite this article as doi: 10.1002/2016GL067861

Abstract

Simulations with a free-running coupled climate model show that heat release associated with Southern Ocean deep convection variability can drive centennial-scale Antarctic temperature variations of up to 2.0°C. The mechanism involves three steps: *Preconditioning:* heat accumulates at depth in the Southern Ocean; *Convection onset*: wind and/or sea-ice changes tip the buoyantly unstable system into the convective state; *Antarctic warming:* fast sea-ice–albedo feedbacks (on annual–decadal timescales) and slow Southern Ocean frontal and sea-surface temperature adjustments to convective heat release (on multidecadal–century timescales) drive an increase in atmospheric heat and moisture transport toward Antarctica. We discuss the potential of this mechanism to help drive and amplify climate variability as observed in Antarctic ice-core records.

Key Points

- Southern Ocean deep convection events can explain up to 2.0°C warming in Antarctica.
- Ocean adjustments to buoyancy loss causes a ~50-yr lag in the Antarctic temperature response.
- Southward atmospheric heat-flux anomalies propagate the warming signal to Antarctica.

1. Introduction

Deep waters rising to the surface along isopycnals in the Southern Ocean (SO) exchange heat and carbon with the global atmosphere [Rintoul and Garabato, 2013]. Intense cooling, sea ice production and wind-driven advection at the SO surface then return these waters to deep and intermediate depths, closing the SO overturning circulation and connecting the atmosphere with the ocean interior [Marshall and Speer, 2012]. It is estimated that ~75% of the ocean store of anthropogenic heat and ~40% of the store of anthropogenic carbon enter the ocean interior through this region [Roemmich et al., 2015; Froelicher et al., 2015]. It follows that past changes in SO overturning could be an important driver of climate variability in Antarctica and the southern high latitudes [e.g. Latif et al., 2013; Menviel et al., 2015].

The dominant mode of deep water production in the modern SO is via brine rejection during sea ice formation on the Antarctic continental shelves [Rintoul and Garabato, 2013]. A second mode, involving deep convection in the open ocean has also been documented [e.g. Gordon, 1991]. In 1974 when the first satellite microwave data was obtained from the Antarctic sea ice zone, a 250,000 km^2 open-ocean polynya was observed in the winter sea ice pack of the Weddell Sea [Carsey, 1980]. The ocean mixed layer in the polynya extended to 3000 m depth, with strong upwelling of relatively warm (with respect to the surface) deep waters, supporting an average winter surface heat flux of 136 Wm^{-2} [Gordon, 1982]. An estimated 2–3 Sv of dense bottom water was produced in the polynya from the intense surface cooling and subsequent deep sinking [Gordon, 1982]. Although initially thought to be a permanent feature, the polynya closed after three years and no open ocean deep convection beyond isolated events lasting some weeks has not been observed since [Gordon, 2014].

While clearly rare in the modern SO, open ocean deep convection may have been more common in the past. Two thirds of IPCC-class global climate models show open ocean deep convection under pre-industrial boundary conditions; the convection shuts down in most of these models in the 21st century due to anthropogenic freshening of SO surface layers [de Lavergne et al., 2014]. Gordon [2014] argues that deep convection was more common in the past and was potentially the dominant mode of SO deep water formation during the glacial when the ice sheets advanced over the Antarctic continental shelf [Golledge et al., 2013], capping the dominant sites of today's deep water formation in the coastal polynyas. The presence of SO deep convection in both observations and climate models raises questions

about the possible climate impacts of shifts between the convective and non-convective modes.

Here we describe an internal mode of SO deep convection variability that causes multicentennial-scale warming events over the Antarctic continent. The mechanism is based on a free-running Kiel Climate Model (KCM) simulation that exhibits deep convection events sharing many similarities with the observed Weddell Sea polynya [Martin et al., 2013]. In the KCM, heat supplied by the lower branch of the Atlantic Meridional Overturning Circulation (AMOC) accumulates in the intermediate depths of the Atlantic-Indian sector of the SO and is then released by deep convection in the Weddell Sea [Martin et al., 2013]. The convection events recur on multicentennial timescales, and feature global teleconnections [Park and Latif, 2008; Latif et al., 2013; Martin et al., 2015]. Each event is associated with sea-ice retreat and a ~2°C sea surface temperature (SST) increase in the convection region (Figures 1a,b and Figure S1).

The onset of deep convection in the KCM requires preconditioning by accumulation of sufficient subsurface heat to make the water column buoyantly unstable; stochastic wind and sea-ice variability then tip the system into the convective state [Martin et al., 2013]. Convection shutdown is linked to stabilization of the water-column by surface freshening from precipitation and sea-ice-melt anomalies. Our mechanism has parallels with the hypothesis of Dokken et al. [2013] in the Nordic seas, in which warm Atlantic waters are isolated beneath a fresh surface layer until halocline collapse, convective overturning and sea-ice retreat drive regional warming.

The overall SO heat loss during convective events in the KCM is of order 10^{23} J (Figure S1), equivalent to one third of the total observed global upper-ocean warming of the last century [Domingues et al., 2008]. We examine the dynamics and timescales by which this ocean heat loss affects surface temperatures over Antarctica and discuss implications for Antarctic climate variability as observed in the paleoclimate record from ice cores.

2. Methods

We use a multimillennial present-day control simulation of the Kiel Climate Model (KCM), an extension of the run in Martin et al. [2015], with constant greenhouse gas forcing (348 ppmv CO_2). The KCM consists of the ECHAM5 atmosphere general circulation model and

the NEMO-LIM2 ocean–sea-ice model applied to a Mercator grid of 2° horizontal resolution with refinement in the tropics and 31 vertical levels [Park et al., 2009]. As the simulation is free-running (i.e. no external perturbations such as freshwater hosing or flux corrections are applied) the deep convection variations are entirely self-sustained. Although the KCM run was conducted under present-day conditions, it could provide insight into SO sea-ice–atmosphere coupling under colder and glacial climate states during which open ocean deep convection is thought to be more prevalent [Gordon, 2014]. We analysed the last 2000 years of the run, which is fully spun-up from the Levitus et al. [1998] climatology.

3. Results

Southern Ocean (SO) deep convection events in the KCM are associated with multicentennial-scale surface air temperature (SAT) variations of ~1.0°C in mean Antarctic temperature and up to 2.0°C at some individual sites where ice core records have been obtained (Figure 1c and Figure S2). The temperature response is strongest in the Atlantic sector of Antarctica and is fastest at near-coastal sites, including Law Dome and James Ross Island. On the Antarctic plateau, the temperature response is more gradual, lagging ~50 years behind the maximum in convection (Figure 1b,c). For example, the simulated temperature at the EDML ice-core site, which is highly correlated with the Antarctic mean temperature (r = 0.90; $p < 0.01$), lags mixed layer depth in the Weddell Sea convective zone by 55 years (r = 0.76, $p < 0.05$).

To investigate the mechanism for Antarctic warming and the cause of the time lag between Antarctic SATs and convective area SSTs, we average the data from the six major convective events. For each event we define two 50-year time slices: “stage 1”, spanning the onset of deep convection and SST increase in the Weddell Sea sector (blue shading, Figure 1); and “stage 2”, spanning the maximum in Antarctic mean SAT (red shading). Composite maps of mean SSTs and SATs for each stage are shown in Figure 2.

During stage 1, the upwelling of warm sub-surface waters results in immediate surface warming in the Weddell Sea sector south of the ACC (Figure 2a); SSTs in the remainder of the SO show very little response. During stage 2 (50–100 years later), vast parts of the Southern Hemisphere have warmed (Figure 2b) in response to the processes triggered by the deep convection in the Weddell Sea. The delayed surface warming north of the ACC reflects the timescale of ocean adjustment to heat and buoyancy loss from the deep convection zone.

Buoyancy loss steepens the meridional ocean density gradient, as evidenced by negative sea-surface height anomalies in the 50˚–70˚S band (Figure 2g). The steeper density gradient causes the ACC to accelerate (Figure 1d) and shift slightly south. The subtropical front shifts south in turn, enabling warm surface waters of the South Atlantic and southern Indian Oceans to expand poleward, and enhancing the transport of warm Indian waters into the Atlantic (Figure 2b). These ocean adjustments contribute to the mid-latitude surface warming that notably occurs in phase with the surface warming over the Antarctic plateau (Figure 1b,c; Figure 2d). AABW export across 30°S also increases by 3–4 Sv in phase with the simulated Antarctic warming (Figure 1d). The timescale of ACC and ocean frontal adjustment to buoyancy forcing in our simulation is consistent with the multidecadal–centennial timescale of ACC adjustment to changes in meridional density gradients [Allison et al. 2011].

The ocean heat transport and frontal adjustments are also coupled to changes in atmospheric circulation and meridional heat transport. At the onset of deep convection, the immediate high-latitude warming in the convective area *reduces* the meridional temperature gradient (Figure 2h, black dashed line), shifting the circumpolar westerlies north of their long-term mean (Figure 2e, red contours). In contrast, the subsequent mid-latitude warming strengthens the meridional temperature gradient and is associated with a poleward intensification of the westerlies (Figure 2f). See also Figure S3 for comparisons of the zonal mean and Atlantic sector meridional SST, sea surface height and wind gradients.

Increased mid-latitude temperatures and more intense polar westerlies are associated with enhanced poleward transport of heat and moisture by atmospheric eddies [e.g. Rind, 2000; Sen-Gupta and England, 2006]. This points to a role for the lagged (stage 2) increase in the mid-latitude temperatures and westerlies in driving the Antarctic warming. We calculate the total meridional heat-transport anomalies during the KCM convection events using zonal averages of the radiation budget at the top of the atmosphere (TOA) and at the surface, surface fluxes of sensible and latent heat, and ocean heat content changes. The schematic in Figure 3 summarizes the resulting heat-transport anomalies (with respect to the long term mean) for the zonal bands 50˚–70˚S and south of 70˚S (where the westerlies and ACC are centered at ~50˚S and the margin of the Antarctic continent is at ~70˚S). The schematic shows separately the heat-flux terms during active deep-convection (stage 1, Figure 3 left panel) and during the maximum in Antarctic warming (stage 2, Figure 3 right panel). The heat-flux terms are also tabulated in Table S1.

During stage 1, the active deep convection results in a 10 TW ocean to atmosphere surface heat-flux (SHF) anomaly over the 50˚–70˚S band. Sea-ice retreat, partly damped by increases in cloud cover, then causes a 5 TW increase in the net downward TOA heat flux. The large transfer of heat from SO intermediate depths to the surface ocean and the sea-ice–albedo feedback support a 13 TW *northward* atmospheric heat-flux anomaly toward the mid-latitudes (contributing to the gradual mid-latitude warming) and a 2 TW increase in the southward atmospheric heat flux across 70˚S to Antarctica (driving some warming at near-coastal ice-core sites). During stage 2, the mid latitudes have warmed and support a 12 TW increase in *southward* atmospheric heat flux across 50˚. The increased southward atmospheric heat flux in combination with ongoing sea-ice–albedo feedbacks then supports a 6 TW increase in the atmospheric heat flux across 70˚S to Antarctica. It is this lagged increase in the southward atmospheric heat flux that explains the lag of the maximum Antarctic warming behind SSTs in the convective area. The southward heat-flux anomalies also correlate with enhanced moisture transport onto the Antarctic continent, resulting in a small (~2%) increase in cloud cover during stage 2 (not shown).

4. Discussion

Heat release from changes in SO overturning is invoked in multiple hypotheses seeking to explain Antarctic climate variations, ranging from centennial-scale variability in SSTs on the western margin of the Antarctic Peninsula [Etourneau et al., 2013; Shevenell et al., 2011] to millennial-scale variability in Antarctic temperatures during the glacial [Weaver et al., 2003; EPICA 2006, Anderson, 2009; Menviel et al., 2015]. Previous studies have primarily considered the response of SO overturning to externally-imposed or remotely-triggered forcings, such as wind stress [Anderson et al., 2009; Lee et al., 2011], changes in deep water production in the North Atlantic [Broecker et al., 1998; Menviel et al., 2015], locally applied meltwater (or salinity) fluxes [Weaver et al., 2003; Menviel et al., 2015] and atmospheric temperature changes [Watson and Garabato, 2006]. Although debate continues on the relative role of such forcings in past (and future) climate variations, a common conclusion is that increased rates of the upwelling of deep waters, which are relatively warm with respect to the surface, lead to SST warming and sea ice retreat.

Missing from previous studies has been analysis of how warming at the SO surface is propagated to the Antarctic continent itself. Our results point to a critical role for amplifying sea-ice feedbacks, movement of ocean fronts and changes in atmospheric heat transport. Also

missing from previous studies has been the concept that variations in SO deep convection may be an intrinsic part of the coupled sea-ice–atmosphere system in the SO. This is not to dispute the influence on Antarctic climate of external forcings or teleconnections from remote locations. Indeed, external forcings could push the SO state toward the convective or non-convective mode, thereby amplifying remote forcings. The presence of such an amplifying mechanism could help to resolve several open questions in the climate dynamics of the southern high latitudes.

The bipolar ocean seesaw mechanism proposes that the centennial-to-millennial-scale Antarctic warming events of the last glacial period — Antarctic Isotope Maxima (AIMs) — result from changes in northward heat transport by the Atlantic Meridional Overturning Circulation (AMOC) modulating SO heat content [Crowley, 1992; Stocker and Johnsen, 2003]. The AIMs occur out of phase with abrupt Dansgaard-Oeschger events in Greenland ice cores (EPICA Community Members, 2006; and see Figure S4); the prevailing view is that a collapsed state of the AMOC reduces northward ocean heat transport in the Atlantic, causing gradual *warming* in the SO and Antarctica at the same time as abrupt *cooling* (amplified by sea ice variations) in the North Atlantic and Greenland (and vice versa for a strengthening of the AMOC) [e.g. Ganapolski and Rahmstorf, 2001; Schmittner et al., 2003]. However, the ocean seesaw mechanism is challenged on physical oceanographic grounds by the difficulty of propagating anomalies between the South Atlantic and Antarctica; the problem is that the Antarctic Circumpolar Current (ACC) presents a dynamic barrier [Ferrari and Nikurashin, 2010] and there is no zonal boundary for wave propagation, leaving eddy fluxes of temperature and salinity or atmospheric teleconnections to propagate the signal across the ACC [e.g. Schmittner et al., 2003; Vettoretti and Peltier, 2015].

Earth-system model studies in which the AMOC strength is abruptly altered generally show strong temperature anomalies in the South Atlantic; the temperature response in the SO and Antarctica is less consistent between models, with a damped temperature response in some [Schmittner et al., 2003; Menviel et al., 2015; Vettoretti and Peltier, 2015; Pedro et al., 2016] and little or no response in others [e.g. see review by Kageyama et al., 2013].

Menviel et al. [2015] argue that AMOC-induced changes in meridional ocean heat transport can drive Antarctic temperature anomalies of order 0.5–1.5°C but are insufficient to account for the 2–3°C increases of Antarctic temperature and SO SSTs reported for the largest Antarctic warming events (e.g. AIM 7 and 8, see Figure S4) [e.g. Parrenin et al., 2013;

Phanke and Sachs, 2006; Barrows et al., 2007; Lopes dos Santos, 2013]. Applying freshwater/salinity anomalies to the SO surface can bring the temperature response in the model in line with observations [Menviel et al., 2015], by directly forcing changes in SO overturning; however, the large fluxes of freshwater required are not well-supported by data.

We suggest that shifts between convective and non-convective modes of the coupled sea-ice–atmosphere system in the SO provide an alternative mechanism to help drive or amplify Antarctic warming events. Support that Antarctic warming events are associated with changes in SO overturning comes from neodymium isotope ratios from South Atlantic marine cores indicating northward advance of Antarctic Bottom Water (AABW) during the Antarctic warming phase [e.g. Piotrowski et al., 2008; Gottschalk et al., 2015]. In our results, AABW export across 30°S increases by 3–4 Sv in phase with the simulated Antarctic warming, while ACC strength increases by ~10 Sv (Figure 2d). Southern Ocean marine sediment records indicate that large AIM events are accompanied by enhanced SO overturning (also ventilating CO_2 from the deep SO) [Anderson et al., 2009; Skinner et al., 2014] and by increases in ACC strength [Lamy et al., 2015].

There are two important challenges to the relevance of our deep convection mechanism to observed AIM events. First, the model warming events have durations of up to 400 years, whereas most AIMs in the ice core record are millennial-scale with only a few examples of centennial-scale events (Figure S4). Second, a complete description of AIM events must account for their systematic relationship with the Dansgaard-Oeschger events in the North Atlantic and also with changes in the position of the Intertropical Convergence Zone (ITCZ) [e.g. Wang et al., 2001; WAIS Divide Project Members, 2015]. We address these challenges in turn below.

The potential for our mechanism to operate over longer timescales is suggested by sensitivity experiments with KCM, which show that deep convection is less frequent under thicker sea ice (and vice-versa); this is because the surface-freshening influence of sea ice requires that more heat accumulate at depth before stratification can be overcome [Martin et al., 2013]. While our simulations were conducted under modern boundary conditions, we hypothesize that the more extensive and thicker sea ice under glacial boundary conditions [Gersonde et al., 2005] may cause deep convection events to occur less frequently and last longer.

The systematic out-of-phase relationship between North Atlantic Dansgaard-Oeschger events

and AIM events calls for a process to push the southern high-latitude system towards the convective (warming) state while the North Atlantic is in the cold (stadial) state, and vice versa. Evidence from climate-proxy and modeling results shows that during the stadial state, the ITCZ and the SO surface wind field are both shifted south [e.g. Wang et al., 2001; Chiang et al., 2014; Montade et al., 2015, Ljung et al., 2015]. Whether changes at low latitudes themselves precede [e.g. Steffensen et al., 2008; Kleppin et al., 2015] or lag [e.g. Huber et al., 2006] changes in the North Atlantic remains unclear. But in either case, southward-shifted winds would indeed be expected to push the SO system toward the convective state by enhancing the Ekman-driven upwelling of intermediate-depth waters, enhancing the advection of sea ice northward away from the convective zone, and by deepening the mixed layer [Hall and Visbeck, 2002; Cheon et al., 2014, Ferrari et al., 2015]. The situation would be reversed in the case of interstadials in which there is evidence (as cited above) for a northward shift in the ITCZ and southern westerlies. It is thus possible that a chain of coupled ocean and atmosphere processes helps to bridge the oceanic barrier formed by the ACC.

5. Summary

In summary, we have shown quantitatively that Southern Ocean (SO) deep convection events can drive temperature variations in Antarctica of up to 2°C. The mechanism can be summarised into the following three steps. (1) *Preconditioning:* heat accumulates at depth in the SO, shifting the water column toward a buoyantly unstable state. (2) *Convection onset*: SO wind-stress and/or sea-ice variability, potentially influenced by atmospheric teleconnections from low latitudes, tip the preconditioned system into the convective state. (3) *Ocean–atmosphere readjustment* on two timescales: first, a fast (annual–decadal) response in which ocean to atmosphere heat flux from convective overturning is amplified by sea-ice–albedo feedbacks, driving immediate increases in SST in the convective zone; second, a slower (multidecadal–century) response in which buoyancy loss from the convective zone forces a southward migration of the ACC and associated SO fronts. The frontal migration combined with atmospheric heat-flux anomalies from the convective zone causes SST increases in the southern mid-latitudes, resulting in a poleward intensification of the westerlies and an enhanced atmospheric heat and moisture transport toward Antarctica. Mean Antarctic warming lags the onset of deep convection by ~50 years owing to the adjustment timescale of the ACC and mid-latitude SSTs. Depletion of the SO heat reservoir

and surface freshening eventually shuts down convective overturning, returning the system to the preconditioning step.

Acknowledgements

T.M. and J.B.P. have equally contributed to this study. J.B.P. and E.J.S. conceived the original idea. T.M. led the analysis and made the figures with feedback from all authors. M.J. provided guidance on the energy balance calculations. W.P. ran the KCM simulations. S.O.R provided input on Dansgaard-Oeschger variability and ice-core dating. J.B.P and T.M. wrote the paper with contributions from all authors. We thank L. Herraiz-Borreguero and participants of the *Ice2Ice* 'Southern Ocean and MIS3' workshop (funded by the European Research Council under the European Community's Seventh Framework Programme (FP7/2007-2013) / ERC grant agreement no. 610055) for stimulating discussions. J.B.P. acknowledges support from the Joint Institute for the Study of the Atmosphere and Ocean (JISAO Contribution No. 2461) and from a Marie Curie International Incoming Fellowship. T.M and W.P acknowledge support from GEOMAR. The model integration was performed at the computing center of Kiel University and model output is available upon request by contacting T.M. or W.P. We thank two anonymous reviewers for their good advice that greatly strengthened the manuscript.

References

Allison, L. C., H. L. Johnson, and D. P. Marshall (2011), Spin-up and adjustment of the Antarctic Circumpolar Current and global pycnocline. *J. Mar. Res.*, *69*, 167–189, doi:10.1357/002224011798765330.

Anderson, R. F., S. Ali, L. I. Bradtmiller, S. H. H. Nielsen, M. Q. Fleisher, B. E. Anderson, and L. H. Burckle (2009), Wind-Driven Upwelling in the Southern Ocean and the Deglacial Rise in Atmospheric CO_2, *Science*, *323*, 1143–1448, doi:10.1126/science.1167441.

Barrows, T. T., S. Juggins, P. De Deckker, E. Calvo, and C. Pelejero (2007), Long term sea surface temperature and climate change in the Australian-New Zealand region, *Paleoceanography*, *22*(PA2215), doi:10.1029/2006PA001328.

Broecker, W. (1998), Palaeocean circulation during the last deglaciation: A bipolar seesaw?, *Paleoceanography*, *13*, 119–121.

Carsey, F. D. (1980), Microwave Observation of the Weddell Polynya. *Mon. Wea. Rev.*, *108*, 2032–2044. doi:10.1175/1520-0493(1980)108<2032:MOOTWP>2.0.CO;2

Cheon, W.G., Y.-G. Park, J.R. Toggweiler, and S.-K. Lee (2014), The Relationship of Weddell Polynya and Open-Ocean Deep Convection to the Southern Hemisphere Westerlies, *J. Phys. Oceanogr.*, *44*, 694–713, doi:10.1175/JPO-D-13-0112.1

Chiang, J.C.H., S. –Y. Lee, A. E. Putnam, and X. Wang (2014), South Pacific Split Jet, ITCZ shifts, and atmospheric north-south linkages during abrupt climate changes of the last glacial period, *Earth Planet. Sci. Lett.*, *406*, 233–246, doi:10.1016/j.epsl.2014.09.012.

Crowley, T. J. (1992), North Atlantic Deep Water cools the Southern Hemisphere. *Paleoceanography*, *7*, 489–497.

de Lavergne, C., J. B. Palter, E. D. Galbraith, R. Bernardello, and I. Marinov (2014), Cessation of deep convection in the open Southern Ocean under anthropogenic climate change, *Nature Clim. Change*, *4,* 278–282, doi:10.1038/NCLIMATE2132.

Dokken, T. M., K. H. Nisancioglu, C. Li, D. S. Battisti, and C. Kissel (2013), Dansgaard-Oeschger cycles: Interactions between ocean and sea ice intrinsic to the Nordic Seas, *Paleoceanography*, *28*, 491–502, doi:10.1002/palo.20042.

Domingues, C. M., J. A. Church, N. J. White, P. J Gleckler, S. E. Wijffels, P. M. Barker, and J. R. Dunn (2008), Improved estimates of upper-ocean warming and multi-decadal sea-level rise, *Nature*, *453*(7198), 1090–1093, doi:10.1038/nature07080.

EPICA Community Members (2006), One-to-one coupling of glacial climate variability in Greenland and Antarctica, *Nature*, *444*, 195–198, doi:10.1038/nature05301.

Etourneau, J. et al. (2013), Holocene climate variations in the western Antarctic Peninsula: Evidence for sea ice extent predominantly controlled by changes in insolation and ENSO variability, *Clim. Past*, *9*, 1431–1446, DOI:10.5194/cp-9-1431-2013

Ferrari, R., and M. J. Nikurashin (2010), Suppression of Eddy Diffusivity across Jets in the Southern Ocean, *J. Phys. Oceanogr.*, *40*, 1501–1519, doi:10.1175/2010JPO4278.1.

Frölicher, T. L., J. L. Sarmiento, D. J. Paynter, J. P. Dunne, J. P. Krasting, M. Winton (2015), Dominance of the Southern Ocean in anthropogenic carbon and heat uptake in CMIP5 models, *J. Climate*, *28*, 862-886, doi:10.1175/JCLI-D-14-00117.1

Ganopolski, A., and S. Rahmstorf (2001), Rapid changes of glacial climate simulated in a

coupled climate model, *Nature*, *409*, 153–158.

Gersonde, R., X. Crosta, A. Abelmann, L. Armand (2005), Sea-surface temperature and sea ice distribution of the southern ocean at the EPILOG last glacial maximum—A circum-antarctic view based on siliceous microfossil record, *Quat. Sci. Rev. 24*(7-9), 869–896, doi:10.1016/j.quascirev.2004.07.015.

Golledge, N. R., et al. (2013), Glaciology and geological signature of the Last Glacial Maximum Antarctic ice sheet, *Quat. Sci. Rev., 78*, 225–247, doi:10.1016/j.quascirev.2013.08.011 .

Gordon, A. L. (1982), Weddell deep water variability, *J. Marine Res., 40*, 199–217.

Gordon, A. L. (1991), Two stable modes of Southern Ocean winter stratification, In: Deep Convection and Deep Water Formation in the Oceans, Eds. P-C Chu and J-C Gascard, *Elsevier Oceanography Series, 57*, 17-35, Elsevier, Amsterdam.

Gordon, A. L. (2014), Oceanography: Southern Ocean polynya, *Nature Climate Change*, *4*(4), 249–250, doi:10.1038/nclimate2179.

Gottschalk, J., L. C. Skinner, S. Misra, C. Waelbroeck, L. Menviel and A. Timmermann, (2015), Abrupt changes in the southern extent of North Atlantic Deep Water during Dansgaard–Oeschger events, *Nature Geosci. 8*, 950–954, doi:10.1038/ngeo2558.

Hall, A., and M. Visbeck (2002), Synchronous variability in the Southern Hemisphere atmosphere, sea ice, and ocean resulting from the annular mode, *J. Clim., 15*, 3043–3057.

Huber, C., M. Leuenberger, R. Spahni, J. Flückiger, J. Schwander, T. F. Stocker, S. Johnsen, A. Landais, and J. Jouzel (2006), Isotope calibrated Greenland temperature record over Marine Isotope Stage 3 and its relation to CH_4, *Earth Planet. Sci. Lett*., *243*(3–4), 504–519, doi:10.1016/j.epsl.2006.01.002.

Kageyama, M. et al. (2013), Climatic impacts of fresh water hosing under Last Glacial Maximum conditions: a multi-model study, *Clim. Past*, *9*, 935–953, doi: doi:10.5194/cp-9-935-2013.

Kleppin, H., M. Jochum, B. Otto-Bliesner, C. A. Shields, and S. Yeager (2015), Stochastic Atmospheric Forcing as a Cause of Greenland Climate Transitions. *J. Climate*, *28*, 7741–7763, doi: http://dx.doi.org/10.1175/JCLI-D-14-00728.1.

Lamy, F., et al. (2015), Glacial reduction and millennial-scale variations in Drake Passage

throughflow, *Proc. Nat. Acad. Sci. USA*, *112*(44), 13496–13501, doi:10.1073/pnas.1509203112

Latif, M., T. Martin, and W. Park (2013), Southern ocean sector centennial climate variability: dynamics and implications for recent decadal trends. *J. Clim.*, *26*, 7767–7782, doi:10.1175/JCLI-D-12-00281.1.

Lee, S.-Y., J. C. Chiang, K. Matsumoto, and K. S. Tokos (2011), Southern Ocean wind response to North Atlantic cooling and the rise in atmospheric CO_2, Modeling perspective and paleoceanographic implications, *Paleoceanography*, *26*, PA1214, doi:10.1029/2010PA002004.

Levitus S., et al. (1998), World Ocean Database 1998, NOAA Atlas NESDIS 18, 346 pp.

Ljung, K., S. Holmgren, M. Kylander, J. Sjolte, N. Van der Putten, M. Kageyama, C. T. Porter and S. Björck (2015), The last termination in the central South Atlantic, Quat. Sci. Rev., *123*, 193–214, doi:10.1016/j.quascirev.2015.07.003.

Lopes dos Santos, R., M. Spooner, T. Barrows, P. De Deckker, J. S. Sinninghe Damsté, and S. Schouten (2013), Comparison of organic (UK37, TEXH 86, LDI) and faunal proxies (foraminiferal assemblages) for reconstruction of late Quaternary sea surface temperature variability from offshore southeastern Australia, *Paleoceanography*, *28*, 377–387, doi:10.1002/palo.20035.

Marshall, J., and K. Speer (2012), Closure of the meridional overturning circulation through Southern Ocean upwelling, *Nat. Geosci.*, *5*(3), 171–180, doi:10.1038/ngeo1391.

Martin, T., W. Park, and M. Latif (2013), Multi-Centennial Variability Controlled by Southern Ocean Convection in the Kiel Climate Model, *Clim. Dyn.*, *40*(7), 2005–2022, doi:10.1007/s00382-012-1586-7.

Martin, T., W. Park, and M. Latif (2015), Southern Ocean Forcing of the North Atlantic at Multi-centennial Time Scales in the Kiel Climate Model, *Deep Sea Res. II*, *114*, 39–48, doi:10.1016/j.dsr2.2014.01.018.

Menviel, L., P. Spence, and M. England (2015), Contribution of enhanced Antarctic Bottom Water formation to Antarctic warm events and millennial-scale atmospheric CO_2 increase, *Earth Planet. Sci. Lett.*, *413*, 37–50, doi:10.1016/j.epsl.2014.12.050.

Montade, V., M. Kageyama, N. Combourieu-Nebout, M. -P. Ledru, E. Michel, G. Siani, and

C. Kissel (2015), Teleconnection between the Intertropical Convergence Zone and southern westerly winds throughout the last deglaciation, *Geology*, *43*(8), 735–738, doi:10.1130/G36745.1.

Park, W., and M. Latif (2008), Multidecadal and multicentennial variability of the meridional overturning circulation, *Geophys. Res. Lett.*, *35*, L22703, doi:10.1029/2008GL035779.

Park, W., N. Keenlyside, M. Latif, A. Ströh, R. Redler, E. Roeckner, and G. Madec (2009), Tropical pacific climate and its response to global warming in the Kiel Climate Model, *J. Clim.*, *22*, 71–92, doi:10.1175/2008JCLI2261.1.

Parrenin F., et al. (2013), Synchronous change of atmospheric CO_2 and Antarctic temperature during the last deglacial warming, *Science, 339*(6123), 1060–1063, doi: 10.1126/science.1226368.

Pedro, J. B. et al. (2016), The spatial extent and dynamics of the Antarctic Cold Reversal, *Nature Geosci.*, *9*, 51–55, doi:10.1038/ngeo2580.

Phanke, K., and J. P. Sachs (2006), Sea surface temperatures of southern midlatitudes 0–160 kyr B.P., *Paleoceanography*, *21*, PA2003, doi:10.1029/2005PA001191.

Piotrowski, A. M., S. L. Goldstein, S. R. Hemming, R. G. Fairbanks and D. R. Zylberberg (2008), Oscillating glacial northern and southern deep water formation from combined neodymium and carbon isotopes, *Earth Planet. Sci. Lett.*, *272*, 394–405, doi:10.1016/j.epsl.2008.05.011.

Rind, D. (2000), Relating paleoclimate data and past temperature gradients: Some suggestive rules, *Quat. Sci. Rev.*, *19*, 381–390.

Rintoul, S.R. and A.C. Naveira Garabato (2013), Dynamics of the Southern Ocean circulation, In Ocean Circulation and Climate: A 21st Century Perspective. Siedler, G., Griffies, S., Gould, J. and Church, J. (eds.), Oxford, GB, *International Geophysics, 103*, 471-492.

Roemmich D., et al. (2015). Unabated planetary warming and its ocean structure since 2006. *Nature Climate Change, 5*, 240-245, doi:10.1038/nclimate2513.

Schmittner, A., O. A. Saenko, and A. J. Weaver (2003), Coupling of the hemispheres in observations and simulations of glacial climate change, *Quat. Sci. Rev.*, *22*, 659–671.

Sen Gupta A., and M. H. England (2006), Coupled ocean–atmosphere–ice response to

variations in the Southern Annular Mode, *J. Clim.*, *19*, 4457–4486, doi:10.1175/JCLI3843.1.

Shevenell, A. E., A. E. Ingalls, E. W. Domack, and C. Kelly (2011), Holocene Southern Ocean surface temperature variability west of the Antarctic Peninsula, *Nature*, *470*, 250–254, doi:10.1038/nature09751

Skinner, L. C., C. Waelbroeck, A. E. Scrivner, and S. J. Fallon (2014), Radiocarbon evidence for alternating northern and southern sources of ventilation of the deep Atlantic carbon pool during the last deglaciation, *Proc. Natl Acad. Sci. USA*, *111*(15), 5480–5484, doi:10.1073/pnas.1400668111.

Steffensen, J. P., et al. (2008), High-Resolution Greenland Ice Core Data Show Abrupt Climate Change Happens in Few Years, *Science*, *321*, 680–684, doi:10.1126/science.1157707

Stocker, T. F., and S. J. Johnsen (2003), A minimum thermodynamic model for the bipolar seesaw, *Paleoceanography*, *18*, PA000920, doi:10.1029/2003PA000920.

Vettoretti, G., and W. R. Peltier (2015), Interhemispheric air temperature phase relationships in the nonlinear Dansgaard-Oeschger oscillation, *Geophys. Res. Lett.*, *42*, 1180–1189, doi:10.1002/2014GL062898.

WAIS Divide Project Members (2015), Precise interpolar phasing of abrupt climate change during the last ice age, *Nature*, *520*, 661–665, doi:10.1038/nature14401.

Wang, Y. J. et al. (2001), A High-Resolution Absolute-Dated Late Pleistocene Monsoon Record from Hulu Cave, China, *Science*, *294*, 2345–2348, doi:10.1126/science.1064618.

Watson, A. J. and A. C. Naveira Garabato (2006), The role of Southern Ocean mixing and upwelling in glacial-interglacial atmospheric CO_2 change, *Tellus B*, *58*, 73–87, doi:10.1111/j.1600-0889.2005.00167.x.

Weaver, A. J., O. A Saenko, P. U. Clark, and J. X. Mitrovica (2003), Meltwater Pulse 1A from Antarctica as a Trigger of the Bølling- Allerød Warm Interval, *Science*, *299*, 1709–1713, doi: 10.1126/science.1081002.

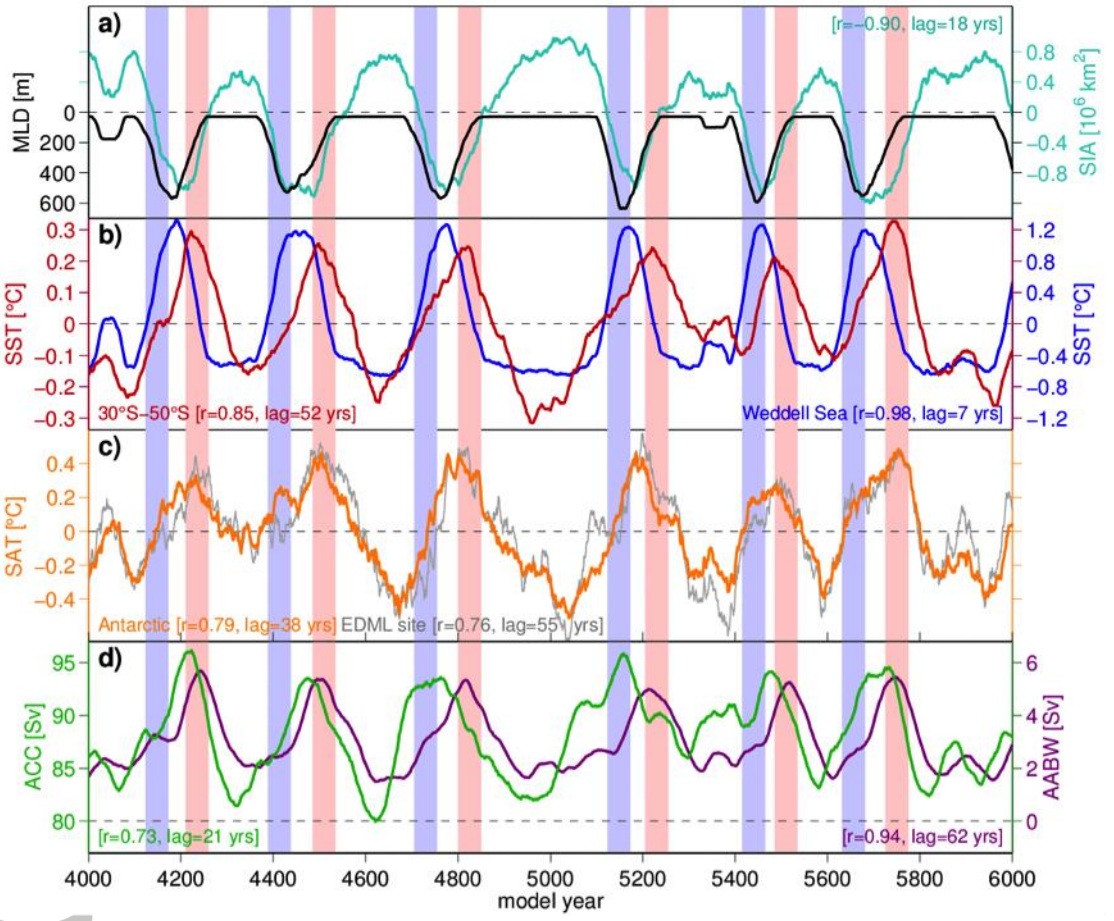

Figure 1: a) Mixed-layer depth (MLD, black) averaged over the Weddell Sea convection region (58–68˚S, 35˚W–10˚E) and total southern hemisphere sea ice area (SIA) anomaly (turquoise). **b)** Mean sea-surface temperature (SST) anomaly for the convection region (blue) and for the zonal band 30–50˚S (red). **c)** Surface air temperature (SAT) anomaly averaged over the Antarctic continent (70–90˚S, orange) and at the location of the EDML ice core (gray). **d)** Drake Passage transport as an indicator of Antarctic Circumpolar Current (ACC) strength (green) and Antarctic Bottom Water (AABW) export across 30°S (purple). All time series are low-pass filtered by applying a 50-year running mean. Lagged correlations between Weddell Sea MLD and each variable are listed inset; in all cases MLD leads and *r* values are significant at $p < 0.05$ (accounting for auto-correlation). Blue shading marks the onset of the convective period (stage 1), and red shading the maximum of subsequent Antarctic SAT (stage 2).

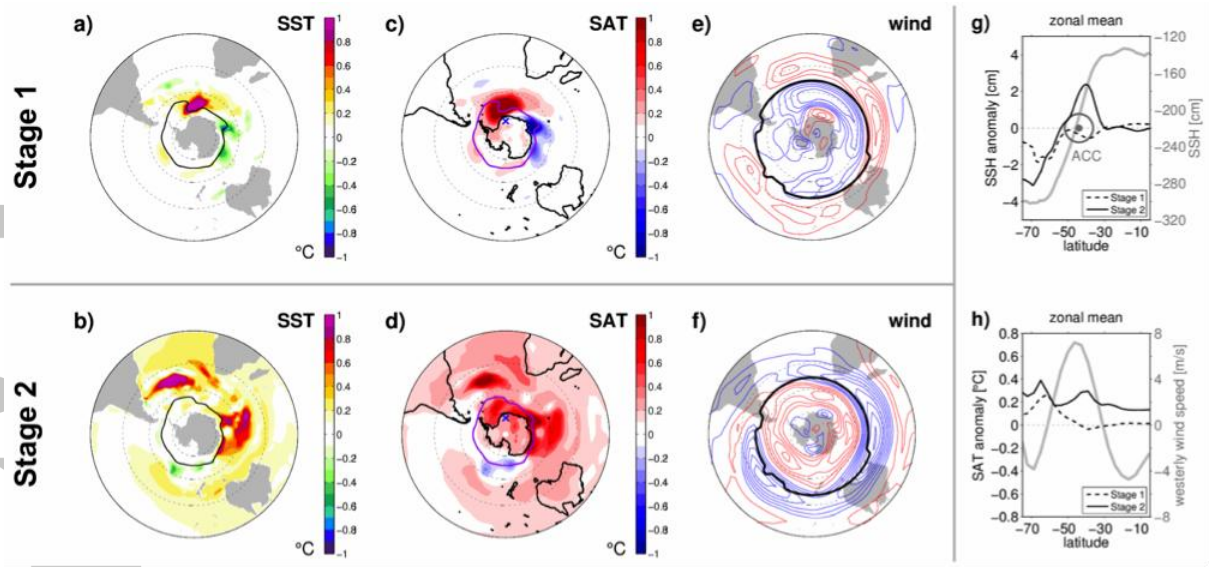

Figure 2: a) Composite sea surface temperature (SST) anomaly for stage 1 (active deep convection). The bold black line indicates the composite mean sea ice edge (15% ice concentration). **b)** Same as (a) for stage 2 (maximum Antarctic warming). **c)** Composite surface air temperature (SAT) anomaly for stage 1. The purple line indicates the sea ice edge and 'x' marks the EDML site on Antarctica. **d)** Same as (c) for stage 2. **e)** Composite of the westerly-only wind speed anomaly at 500 hPa (U_{500}>0 m/s) for stage 1, with red contours depicting positive wind speed anomalies in 0.05 m/s increments (blue contours negative). The bold black line highlights the latitude of maximum long-term mean westerly wind speed. **f)** Same as (e) for stage 2. **g)** The zonal mean sea surface height (SSH) anomaly for stage 1 (black dashed line) and stage 2 (black solid line), with the long-term zonal mean SSH relative to the global mean shown overlain (grey line, axis on right). The black bullseye marks the zonal mean latitude of the ACC. **h)** The zonal mean SAT anomaly for stage 1 (black dashed line) and stage 2 (black solid line), with the long-term mean westerly 10-m wind speed shown overlain (grey line, axis on right). In all maps the 50˚S and 70˚S latitude circles are marked by thin dashed lines.

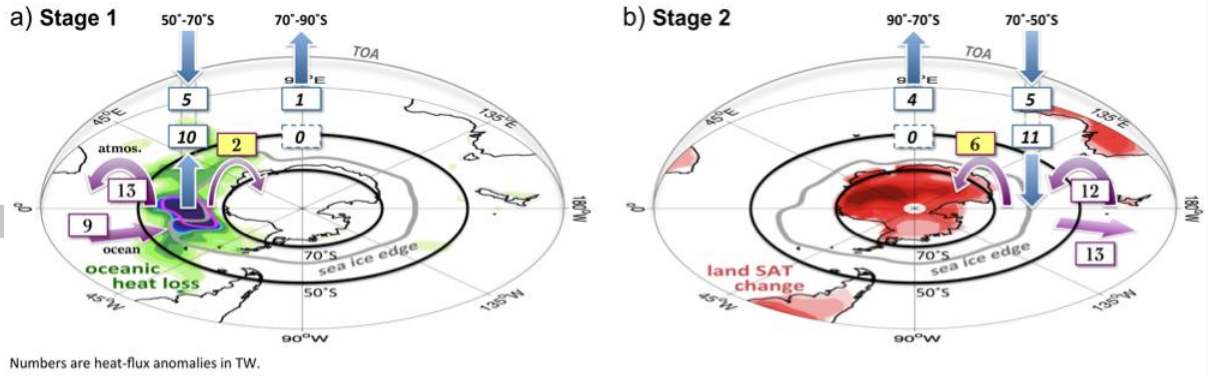

Figure 3: Schematic of the annual mean heat-flux anomalies during the two-stage Antarctic warming process. **a)** Stage 1, active deep convection, with ocean heat loss depicted by green and blue shading, the sea ice edge in gray, and the 200 m mixed-layer depth isoline in magenta (indicating the deep convection area). **b)** Stage 2, maximum in Antarctic warming, surface air temperature changes over land depicted by red shading. For both stages vertical blue arrows and boxes give the direction and strength of anomalies in top of atmosphere (TOA) and surface heat fluxes averaged over latitude bands 50–70˚S & 70–90˚S. Curved purple arrows show the direction and strength of atmospheric zonal mean meridional heat-flux anomalies across 50˚S and 70˚S; horizontal purple arrows show the same for the ocean at 50˚S. Note the increase in southward meridional atmospheric heat transport during stage 2. See Table S1 for additional details and conversion to units of Wm^{-2}.